RSC Advances

PAPER

View Article Online
View Journal | View Issue

Check for updates

Cite this: *RSC Adv.*, 2025, **15**, 5344

Casein-based film enriched with lignin as a biodegradable substrate for enzyme immobilization†

Elena Dembech, [a] Giovanna Sotgiu, [bc] Anna Donnadio, [d] Sara Buoso, [bc] Giovanni Dolci, [e] Mary Jo F. A. Nichilo [e] and Valentina Sinisi *[a]

In the last decades, the negative impact of petroleum derived materials on the environment is more and more evident; beyond the unavoidable reduction in the use of classical plastic, another promising approach is the development of alternative materials prepared starting from natural, biodegradable, and more sustainable biomolecules, particularly undervalued or discarded ones. Caseins are the most abundant proteins in milk, with important nutritional value but also interesting film-forming properties. Lignin is a polyphenolic polymer found in wood and derived from a by-product of the cellulose extraction processes; it is well known for its antibacterial, antioxidant, and UV-protecting properties. In the present work, casein was isolated from UHT skimmed bovine milk through acidification and used alone or in combination with lignin to produce films that are biodegradable and environmentally friendly. Casein and casein-lignin films presented a thickness in the range of 180–260 μm and a compact, non-porous texture. The presence of lignin did not affect the morphology of the films but influenced their mechanical properties. For casein and casein-lignin films covalently crosslinked with transglutaminase (TGM), the solubility decreased to 40–50% and the samples retained their shape. The results show that TGM-containing films are suitable as substrates for the immobilization of enzymes; herein, the FAD-dependent glucose oxidase from *Aspergillus niger* was added to the film and the enzyme remained stable and active against glucose for weeks, as demonstrated by the colorimetric detection of the H_2O_2 produced in the catalysed reaction. This study opens up the possibility of combining two products of natural origin for the production of films through processes with low environmental impact, thus offering interesting scenarios in the immobilization of macromolecules for the detection of target molecules.

Received 3rd December 2024
Accepted 12th February 2025

DOI: 10.1039/d4ra08521c

rsc.li/rsc-advances

Open Access Article. Published on 18 February 2025. Downloaded on 3/12/2025 4:19:18 PM.
This article is licensed under a Creative Commons Attribution-NonCommercial 3.0 Unported Licence.

1. Introduction

The protein content in 1 L of bovine milk is about 32 g, whose 80% is composed of caseins.[1] Caseins are a family of four types of phosphoproteins, known as α_{s1}-, α_{s2}-, β-, and κ-casein,[2,3] that are present in milk as colloidal micelles and precipitate at a pH of about 4.6,[3–5] so they can be isolated through milk acidification.[6] The casein micelles, with an average dimension of 150 nm, scatter the light and this contributes to the white colour of the milk.[7] For human nutrition, caseins are a source of amino acids and minerals, particularly calcium phosphate which is associated with the micelles.[1,3] Besides their important dietary and nutritional value, caseins are particularly interesting from a materials science point of view for their film-forming property, which allows the production of casein-based materials with various applications. Several examples are reported in the literature: casein-based coatings and films for food preservation,[8–10] hydrogels for drug delivery and controlled release,[11–14] materials for wound treatment,[14–18] adhesives,[19,20] films and hydrogels for sensors.[14,21,22]

Lignin is a natural, three-dimensional, polyphenolic polymer and it is one of the three main constituents of lignocellulosic biomass, together with cellulose and hemicellulose. Lignin has a complex structure given mainly by the cross-linking of three phenolic units, *i.e.* coniferyl, *p*-coumaryl, and sinapyl alcohols; moreover, its composition in plants depends on the type of

[a]*Institute of Materials for Electronics and Magnetism, National Research Council (CNR-IMEM), Parco Area delle Scienze, 37/A, 43124 Parma, Italy. E-mail: valentina.sinisi@cnr.it*

[b]*Institute for Organic Synthesis and Photoreactivity, National Research Council (CNR-ISOF), Via P. Gobetti, 101, 40129 Bologna, Italy*

[c]*Kerline Srl, Via P. Gobetti, 101, 40129 Bologna, Italy*

[d]*Department of Pharmaceuticals Sciences, University of Perugia, Via del Liceo 1, 06123 Perugia, Italy*

[e]*Politecnico di Milano, Department of Civil and Environmental Engineering, Environmental Section, Piazza Leonardo da Vinci 32, 20133 Milano, Italy*

† Electronic supplementary information (ESI) available: LCA data, UV-Vis spectrum of casein; DLS and *Z*-potential data; NMR of casein; average thickness, solubility and biodegradability data of films; XRD diffractograms; optical microscope images; further SEM images; mechanical properties data; LCA results; FT-IR and SEM images of GOx-containing films; graph reporting the activity of GOx in solution, and of GOx entrapped in the films during time. See DOI: https://doi.org/10.1039/d4ra08521c

© 2025 The Author(s). Published by the Royal Society of Chemistry

Open Access Article. Published on 18 February 2025. Downloaded on 3/12/2025 4:19:18 PM.
This article is licensed under a Creative Commons Attribution-NonCommercial 3.0 Unported Licence.

plant tissue and on the plant type, but also on the environmental conditions.[23,24]

The basic functions of lignin are to mechanically reinforce the plant cells and organs, to allow the flux of water inside the plants, and to protect the plants from pathogens and UV damages, thanks to its antibacterial, antioxidant, and anti-UV properties.[23,24] Every year, lignin is produced in large quantities as a component of the black liquor, a by-product of the cellulose extraction processes, necessary for example for the paper manufacturing; the paper industry alone produces more than 50 million tons of lignin per year worldwide.[25] For a long time, lignin was undervalued, being manly utilised to produce energy by burning; however, in the last decades the scientific interest in lignin valorisation strongly increased due to its huge abundance, low cost, natural origin, sustainability, and useful properties, making it a promising starting biopolymer to develop added value products.[25–27]

In the present paper, we describe the development of casein-based films enriched with lignin. Mattinen *et al.* already proposed lignin nanoparticles coated with β-casein;[28] however, to the best of our knowledge this is the first example of addition of lignin to casein film matrix. In our work, the term casein generally refers to the isolated acid precipitate of Ultra High Temperature (UHT) skimmed bovine milk. The UHT process has a negligible effect on the conformation of the caseins, because such proteins do not have secondary and tertiary structure.[29] The isolation of the casein fraction from milk was chosen in order to work with a truly natural source. From a circular economy perspective, indeed, the protocols described here could be applied to the casein fraction of expired UHT milk, leading thus to the valorisation of a potential waste. Although the UHT processing allows to increase the shelf life, the share of milk wasted before the sale can be higher than 10%.[30,31] The addition of lignin, derived from an industrial by-product, is coherent with the approach of waste valorisation. Moreover, the formulation of these films was studied to be based on safe compounds.

The developed films were tested as substrates for enzymes; in particular, we chose the FAD-dependent glucose oxidase (GOx) from *Aspergillus niger*. GOx catalyses the redox reaction that oxidizes glucose in gluconic acid and releases a molecule of hydrogen peroxide in the presence of molecular oxygen;[32] due to its high specificity against glucose and its stability, it is largely used in enzymatic glucose sensors.[33–35] The activity of the enzyme entrapped in the substrate was evaluated with a colorimetric test,[36] adapted to our experimental conditions, which allows the glucose detection by the naked eye: by soaking a small piece of GOx-containing film, the presence of glucose in a solution could be detected by a visible colour change, from colourless to yellow, due to the reaction between hydrogen peroxide, released in the enzymatic reaction, and KI.

The results presented in our work highlight that the entrapped GOx was still functional and remained active for weeks; the casein-based films are therefore suitable as substrates for enzymes; in particular, if GOx is replaced by other specific oxidases (like lactate or lysyl oxidases), it is also possible to carry out the same colorimetric detection of the analyte of interest.

2. Materials and methods

2.1 Materials

Casein was isolated by precipitation from commercial UHT skimmed bovine milk, bought in a local supermarket and produced by Latteria Soresina Soc. Coop. Agricola (Soresina, Cremona, Italy) from Italian milk. Lignin was purchased from Sigma-Aldrich (lignin alkali 471 003, hereafter mentioned as "lignin Sigma", average MW 10 000 g mol^{-1}; for a further characterization see D'Orsi *et al.*)[37] or kindly provided by UPM-Kymmene Company (kraft lignin UPM BioPiva™ 395GR, hereafter mentioned as "lignin UPM", average MW 6000 g mol^{-1}; for a further characterization see Gazzurelli *et al.*);[38] glycerol from Carlo Erba; potassium dihydrogen phosphate (KH_2PO_4), dipotassium hydrogen phosphate (K_2HPO_4) from Fluka Chemicals; sodium hydroxide (NaOH), glucose oxidase (GOx) from *Aspergillus niger* (type VII, lyophilized powder), peroxidase (POD) type VI from horseradish, and D-(+)-glucose from Sigma-Aldrich; citric acid (CA) from VWR; microbial meat glue transglutaminase (TGM), food grade, from Special Ingredients; potassium iodide (KI) from Rudi Pont S.P.A.; phosphate-buffered saline (PBS) tablets from Fisher Bioreagents. SDS-PAGE electrophoretic precast gels (stacking gel 4%, running gel 20%) and protein standard marker were purchased from BioRad. Glycin (gly), sodium dodecyl sulfate (SDS), tris-base, bromophenol blue, gel staining reagent and acetic acid were purchased from Sigma-Aldrich. Dithiothreitol (DTT) was purchased from TCI Tokyo Chemical Industry. Protease from *Streptomyces griseus* type XIV was purchase from Merck.

2.2 Casein isolation by precipitation

Casein was isolated by precipitation from commercial Ultra High Temperature (UHT) skimmed milk. 500 mL of milk was stirred vigorously on a heated magnetic plate until it reached 52 °C. Caseins were precipitated by adding 50 mL of commercial white wine vinegar. The protein precipitate was poured onto a steel strainer, filtered to remove lipids and sugars, and washed with about 200 mL of distilled water. The ivory-white sediment was placed in a glass crystallizer and dried overnight at room temperature, then it was stored in the fridge in a sealed container.

To evaluate the residual humidity, a small amount of the protein precipitate was heated in a stove at 90 °C for approximately 3 hours, or until the weight became stable. The percentage of humidity in the sample was calculated from the weight difference before and after heating, using the following formula:

$$\text{Hum}\% = (\text{initial weight} - \text{final weight})/\text{initial weight} \times 100 \quad (1)$$

2.3 Film formulation

2.3.1 Casein-based film preparation. 3 or 4 g of isolated casein (the weighted amount depended on the residual humidity of casein and was set to have about 1.3 g of dried

Open Access Article. Published on 18 February 2025. Downloaded on 3/12/2025 4:19:18 PM. This article is licensed under a Creative Commons Attribution-NonCommercial 3.0 Unported Licence.

protein) and 0.5 g of glycerol were dissolved in 15 mL of freshly prepared 0.065 M KH_2PO_4/K_2HPO_4 buffer (pH 8). The prepared solution was magnetically stirred until homogeneity. Lignin, previously solubilized, and/or 250 mg TGM were incorporated into the solution, according to the different sample composition (see Table 1). Before adding TGM, the solution was cooled down to room temperature to prevent enzyme denaturation and inactivation.

Final solutions were cast into 100 mm diameter PTFE Petri dishes, dried overnight at room temperature, followed by 3 hours at 70 °C in stove. Each sample was prepared three times.

2.3.2 GOx-containing film preparation. Two kinds of GOx-containing films were prepared by following the same recipe and procedure described for CT and CS100T except for halving all the amounts and adding a quantity of GOx powder in the end of the preparation. 1.5 or 2 g of isolated casein and 250 mg of glycerol were dissolved in 8 mL of 0.065 M freshly prepared KH_2PO_4/K_2HPO_4 buffer at pH 8.0 (phosphate buffer). The prepared solution was magnetically stirred until homogeneity. Sample CT–GOx was prepared incorporating 15 mg of GOx (dissolved in 1 mL of phosphate buffer) and 125 mg of TGM; for sample CST–GOx, 50 mg of lignin Sigma dissolved in 350 μL of phosphate buffer was incorporated, then 15 mg of GOx (in 1 mL of phosphate buffer) and 250 mg of TGM. Before the addition of GOx and TGM, the solution was cooled down to room temperature to avoid enzyme denaturation and inactivation. Final solutions were cast into 65 mm diameter PTFE Petri dishes, dried overnight at room temperature, and then placed in a stove at 35/40 °C for at least 6 hours. GOx-containing film samples have been prepared in smaller PTFE Petri dishes to combine the need to have a concentrated enzyme in the film with the practical need to use a reduced amount of enzyme due to its commercial cost.

2.4 Characterization

2.4.1 SDS PAGE. SDS-PAGE analysis was performed according to the Laemmli method.[39] 15 μL of the solution of casein 1 mg mL^{-1} (total amount of casein 15 μg) was mixed with 15 μL of denaturing buffer. The mixture was heated at 95 °C for 5 minutes and loaded on the polyacrylamide gel (4% stacking gel, 20% running gel) together with a standard protein marker, soaked in a TRIS/gly/SDS buffer. The voltage during the electrophoresis run was set at 200 V and was supplied by PowerPac™ Basic Power Supply (Bio-Rad).

2.4.2 DLS. Dynamic light scattering (DLS) analysis was performed at 25 °C using a NanoBrook Omni Particle Size Analyzer (Brookhaven Instruments Corporation) equipped with a 35 mW red diode laser (nominal 640 nm wavelength). Samples were analysed in backscattering technique. Casein was dispersed in distilled water at a concentration of 2 mg mL^{-1}. 20 μL of the dispersion was diluted in 3 mL of water, to get a concentration of about 13 μg mL^{-1}. 20 μL of NaOH 5 M was added to avoid larger aggregates and obtain reliable measurements. The reported data are an average of four replicate measurements. The mean effective hydrodynamic diameter and the mean polydispersity are values calculated by the software of the instrument NanoBrook Particle Solutions Software that uses internal algorithms to extrapolate data from the measurement.

2.4.3 Zeta potential. *Z*-potential was performed by phase analysis light scattering (PALS) at 25 °C using a NanoBrook Omni Particle Size Analyzer (Brookhaven Instruments Corporation) equipped with a 35 mW red diode laser (nominal 640 nm wavelength). The samples analysed were the same as those prepared for the DLS measurements, without the addition of NaOH. The reported data are an average over five repeated measurements.

2.4.4 FT-IR. Infrared (IR) spectra were recorded with an Agilent Cary 630 FTIR spectrophotometer equipped with an ATR accessory (diamond), range 4000–650 cm^{-1}. A small aliquot of dry powder, or a drop (for glycerol), or a piece of film was placed on the ATR equipment and pressed, then the FT-IR spectrum was acquired directly using Agilent Microlab FT-IR software.

2.4.5 UV-Vis. Absorbance spectra were acquired with a JASCO V-770 spectrophotometer, using rectangular transparent quartz cuvettes with an optical path of 1 cm, in the wavelength range 250–700 nm. Casein was solubilized in phosphate buffer to approximate the absorbance of 1.

2.4.6 NMR. 30 mg of isolated casein was dissolved in 1 mL of DMSO-D_6 (deuterated). The solution was then transferred to a 5 mm NMR tube. The ^1H NMR spectrum was acquired using an Agilent DD2 NMR System spectrometer operating at a frequency of 500 MHz. The spectrum was recorded at a temperature of 25 °C.

2.4.7 Film thickness. Film thickness was measured for each sample using a handheld micrometer (Mitutoyo). Ten

Table 1 Samples composition (before the addition, lignin Sigma was solubilized in 0.7 mL of distilled water, lignin UPM in 0.7 mL of NaOH 0.5 M)

Sample	Casein	Glycerol	NaOH 0.5 M (0.7 mL)	Lignin Sigma	Lignin UPM	TGM
C	X	X	X			
CT	X	X				X
CS50	X	X		X (50 mg)		
CS100	X	X		X (100 mg)		
CU50	X	X	X		X (50 mg)	
CU100	X	X	X		X (100 mg)	
CS50T	X	X		X (50 mg)		X
CS100T	X	X		X (100 mg)		X
CU50T	X	X	X		X (50 mg)	X
CU100T	X	X	X		X (100 mg)	X

© 2025 The Author(s). Published by the Royal Society of Chemistry

Open Access Article. Published on 18 February 2025. Downloaded on 3/12/2025 4:19:18 PM.
This article is licensed under a Creative Commons Attribution-NonCommercial 3.0 Unported Licence.

random points were considered for each film and used to calculate the average thickness.

2.4.8 Film solubility. The solubility of the film in water was determined using a method adapted from Khan *et al.*[40] For each sample three small squares (about 0.5 cm × 0.5 cm) were weighed. One was put in 1 mL of distilled water, one in 1 mL of PBS buffer (1×, pH 7.4), the last one soaked in 0.5 M citric acid then placed in 1 mL of distilled water. All experiments were performed in 1.5 mL volume centrifuge tubes. The squares were left in the liquid overnight at room temperature. The next day, the undissolved residues of the squares were collected by pouring the contents of the tubes onto filter paper and drying them in a stove at 95 °C for two hours, then the residues were left overnight at room temperature and weighed again on the next day. The film solubility was calculated using the formula:

$$\text{Solub}\% = (\text{initial weight} - \text{final weight})/\text{initial weight} \times 100 \quad (2)$$

2.4.9 Film biodegradability. To evaluate the biodegradability of the films, a 0.5 mg mL^{-1} solution of protease XIV was prepared in PBS 1× pH 7.4. Samples were weighed, immersed in 2 mL of this solution and placed in stove at 37 °C. At regular time intervals (1, 3, 6 and 8 hours), enzymatic digestion was evaluated by thoroughly washing the films with distilled water, drying them in a stove at 50 °C and weighing them and re-dipping them in fresh protease solution.

The percentage of weight loss (W loss%) was calculated using the same formula used for solubility test eqn (2).

$$W\ \text{loss}\% = (\text{initial weight} - \text{final weight})/\text{initial weight} \times 100 \quad (3)$$

2.4.10 XRD analyses. XRD analyses were performed on 1.5 cm × 1.5 cm squares of the films, fixed with double-sided tape on a glass sample holder. The XRD diffractograms were acquired using a Rigaku Miniflex 600 instrument, in the 2θ range 10–60°, step of 0.01°, speed of 10° min^{-1}.

2.4.11 Optical microscope. The samples were directly placed on a microscope slide and analysed with a Nikon Microphot-FXA microscope, with magnification (MAG) from 5× to 40×.

2.4.12 SEM analyses. Small triangles of the samples were placed on carbon tape and coated with gold for 30 seconds (Edward Scancoat Pirani 501). The images were taken with FESEM/FIB ZEISS Auriga Compact instrument, using a secondary electron (SE2) detector, EHT 3 kV, working distance (WD) between 7 and 8 mm.

2.4.13 Mechanical properties. The mechanical properties of the films were determined by the tensile tests, with a Zwick Roell Z1.0 testing machine, with a 200 N static load cell using at least three replicates. The films were cut into rectangles 5 mm wide and 50 mm long and fixed on the grips of the device with a gap of 20 mm. The thickness of the sample, determined with an uncertainty of ±5 μm, was in the range of 200–210 μm in the measured portion. Prior to texting, the films were stored for one week at 23 ± 2 °C above 33% relative humidity and then tested at a speed of 100 mm min^{-1}. The data were elaborated by the TestXpert V11.0 Master software.[41] The Young's modulus (E) was calculated from the linear part of the stress–strain curve, in the range 0.2% and 0.6% of elongation. The standard deviation resulting from the analysis of at least three film stripes for each sample was considered for statistical analysis.

2.4.14 Life cycle assessment (LCA). A comparative LCA was performed to quantify and compare the potential environmental impacts associated with the production of the different film samples. The LCA methodology was applied in accordance with the principles outlined in the current international technical regulations, specifically the standards ISO 14040 (ref. 42) and ISO 14044.[43] The functional unit was defined as one unit of film. The system boundary extends from raw material extraction to film production, representing a "cradle-to-gate" analysis. The modelling of the films and the subsequent environmental impact assessments were performed by using the SimaPro software (9.6.0.1 version, PRéSustainability, Amersfoort, The Netherlands). The assessment examined the 16 midpoint impact categories included in the Environmental Footprint 3.1. Normalization and weighting were also performed according to the factors specified in the same method.[44]

The system under investigation was mainly described using primary inventory data, supplemented by secondary data where necessary (from Tables 1-SI–16-SI†). The analysis was supported by the ecoinvent database (version 3.10 allocation, cut-off by classification system model).[45] The selection of the geographical locations of the datasets prioritized the Italian and European contexts, and where necessary, global geographical context.

2.5 Glucose detection with GOx

The enzymatic oxidation of D-glucose to gluconic acid in the presence of molecular oxygen determines the formation of hydrogen peroxide (H_2O_2) and it is catalysed by the FAD-dependent glucose oxidase (GOx) from *Aspergillus niger*. The oxidation of glucose proceeds enzymatically since the enzyme contains the cofactor FAD which accepts electrons from glucose and transfers them to molecular oxygen. During the reaction, FAD molecule is regenerated, allowing the enzyme to accept other glucose molecules. The GOx-mediated production of H_2O_2 was monitored by adding KI to the reaction mixture and following the formation of the stable yellow triiodide ion (I_3^-), which is generated as a reaction product of the chemical reaction between KI and H_2O_2. Variations in absorbance at the fixed wavelength of 350 nm, corresponding to the formation of I^{3-}, were recorded at 25 °C using a JASCO V-770 spectrophotometer. Reactions were prepared in a transparent quartz cuvette by mixing different concentrations of the reagents and placing a 5 mm × 6 mm piece of casein-based films containing GOx (CT–GOx and CST–GOx) on the bottom of the cuvette. The reaction mixture contained 40 mM KI in PBS buffer, pH 7.4, and was started by the addition of 10 mM D-glucose. D-fructose was used as an interferent instead of D-glucose to ensure that the increase in the absorbance was related to the enzymatic production of H_2O_2.

Open Access Article. Published on 18 February 2025. Downloaded on 3/12/2025 4:19:18 PM. This article is licensed under a Creative Commons Attribution-NonCommercial 3.0 Unported Licence.

To confirm the maintenance of the glucose oxidase activity for the immobilized enzyme in the film and to compare the enzymatic activities for different gels, the release of H_2O_2 was monitored spectrophotometrically at 350 nm by using a continuous coupled assay with 5 μM POD (peroxidase, from horseradish) and an excess of KI. POD is a heme-dependent enzyme which oxidizes colourless organic or inorganic compounds using hydrogen peroxide as the electron acceptor, releasing a water molecule and an oxidized product that emits into the visible.[46] Since POD oxidizes KI to the yellow-coloured I^{3-} with the H_2O_2 produced by GOx, the occurrence of the POD reaction allows monitoring of GOx enzymatic activity in the enzymatic coupled assay.[47] The excess of the coupled enzyme POD ensures a rapid formation of I^{3-} thus allowing the comparison of GOx enzymatic reactions under different conditions.

The kinetics of either immobilized or free GOx were determined at room temperature in the presence of POD and an excess of D-glucose concentration; intervals of 30 seconds were considered to measure the slope of the absorbance signal and to estimate the corresponding initial velocities V_0 using the I^{3-} extinction coefficient (21 000 M^{-1} cm^{-1})[48] in the presence of 1 μM GOx.

The enzymatic assay with KI and POD was repeated in duplicate during the forty-eight days after the preparation of the films, and the maintenance of the enzymatic activity was evaluated on different squares (0.5 cm × 0.5 cm) cut from the films stored at 4 °C.

3. Results and discussion

3.1 Casein isolation and characterization

The isolation of casein by precipitation from UHT skimmed milk occurred quickly: after the addition of vinegar to the heated milk, a large amount of granular precipitate appeared in few minutes; it could be easily isolated from the whey through filtration, washed and left to dry overnight (Fig. 1A). The amount of isolated casein from 500 mL of milk was 42 g on average, with a residual humidity in the range 53–67%. Stored in a refrigerator, the isolated casein could last as long as one month.

The FT-IR spectrum (Fig. 1B) showed a broad band with the maximum at 3274 cm^{-1}, which is the result of the OH and NH stretching absorptions; the signals at 2931 cm^{-1} is due to the CH stretching; the peaks at 1629 and 1509 cm^{-1} are typical for the amidic backbone of casein, and they raise from the C=O stretching and the sum of C–N stretching and NH bending, respectively; the signals at 1439 and 1232 cm^{-1} are attributable to the C–H and NH deformation; the peak at 1055 cm^{-1} is due to the C–O stretching.[49]

The UV-Vis spectrum (Fig. 1-SI†) of the isolated casein showed the typical absorbance peak at 280 nm of the aromatic groups of the amino acids tryptophan, tyrosine, and phenylalanine, present in casein sequences.[3]

The SDS-PAGE (20%) confirmed the expected molecular weights for the isolated casein proteins. A strong pattern with two major bands can be detected between 25 and 37 kDa and less visible bands at 17–18 kDa (Fig. 1C), corresponding to the populations of α-, β-, and κ-caseins present in bovine milk.[50]

The DLS performed on casein dispersed in water with the addition of NaOH 5 M (Table 17-SI†) indicated a mean hydrodynamic diameter of 994.11 ± 56.20 nm and a high polydispersity value of 0.419 ± 0.026, some sedimentation phenomena can be detected (correlation graph in Fig. 2-SI†). The negative *Z*-potential of 19.14 ± 0.34 mV (Table 18-SI†), measured in water, was expected due to the anionic charge of the isolated casein.[51]

The ^1H NMR spectrum of casein in DMSO-D_6 (Fig. 3-SI†) showed a number of characteristic signals reflecting the complex structure of casein, which is composed of several protein fractions, including α_{s1}-, α_{s2}-, β- and κ-casein, each of which contributes to the NMR spectrum. In particular, signals in the region between 0.5 and 2.5 ppm are typical of the protons of the methylene and methyl groups of aliphatic amino acids such as leucine, isoleucine and valine. The signals between 2.5 and 4.5 ppm are attributed to the α protons of amino acids and the protons of amide groups. Signals in the region between 6 and 8 ppm are attributable to the aromatic protons of amino acids such as phenylalanine and tyrosine.[52,53]

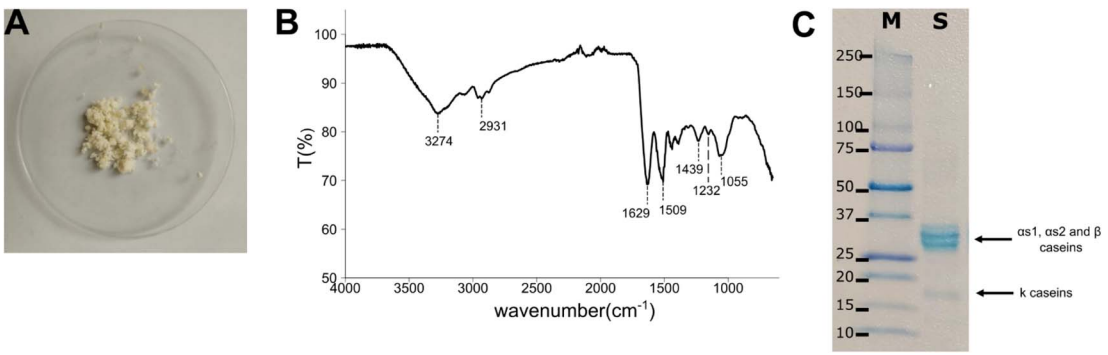

Fig. 1 (A) Photograph of the casein isolated by precipitation after overnight drying at room temperature, (B) FT-IR of casein: relevant signals are highlighted with dotted lines, (C) SDS-PAGE analysis (20%) of isolated proteins from UHT skimmed milk: (M) marker, and (S) isolated sample. Casein bands present in S are pointed with black arrows.

© 2025 The Author(s). Published by the Royal Society of Chemistry

Open Access Article. Published on 18 February 2025. Downloaded on 3/12/2025 4:19:18 PM.
This article is licensed under a Creative Commons Attribution-NonCommercial 3.0 Unported Licence.

3.2 Casein film preparation

To prepare the casein-based films, at first casein and glycerol were solubilized in phosphate buffer (pH 8.0): to speed up the protein solubilization, it was necessary to warm the mixture to about 70 °C. Before being added, lignin Sigma was solubilized in water, resulting in a dark brown solution with pH 8–9, while lignin UPM needed to be solubilized in 0.5 M NaOH because it is not soluble only in water. In the films containing TGM, the enzyme was added to the cooled mixture as a powder; the addition was slow to avoid as far as possible the formation of lumps difficult to be homogenised.

The drying in the stove after the overnight one at room temperature was a crucial step: the further reduction of the residual humidity allowed to prevent the films from getting mouldy, so they could be stored in sealed plastic bags at room temperature, even for months. Once dried, the films could be easily detached from the PTFE Petri dish, using a flat spatula as a lever.

The films were smooth and quite flexible; the colour depended on the components: ivory without lignin, chestnut with both kinds of lignin (Fig. 2).

3.3 Casein film characterization

3.3.1 Thickness, solubility, biodegradability. The films' thickness was in the range of 180–260 μm, with a variability among the samples due to the specific film composition; the average thickness of each sample, determined as the average of the measurements in ten random points, is reported in Table 19-SI.†

The solubility in water depended on the kind of sample (Table 20-SI and Fig. 4-SI†): without TGM, the films appeared to be less resistant to water with a solubility in the range of 70–80%, when measurable; moreover, they lost their shape, tending towards the dissolution; with TGM, on the other hand, the solubility dropped down to 40–50% and the samples retained their shape, with a clear swelling. Such result was predictable since TGM is an enzyme that catalyses the formation of covalent bonds between the γ-carboxyamide group of glutamines and the ε-amino group of lysines or free amino groups, allowing the formation of isopeptide bonds between the side chains of proteins, resulting thus in a more stable protein matrix.[54]

Due to the possible application as substrate for enzymes, the solubility of the films was also evaluated in PBS 1× pH 7.4: the trend was coherent with that obtained in distilled water, showing a quite good resistance for the samples crosslinked by TGM, with an average solubility of about 40%.

A further test was performed soaking the samples in 0.5 M citric acid before leaving them in water overnight; the acid treatment was added considering that casein is almost insoluble at low pH. The results showed that citric acid had a limited impact on improving water resistance in the samples crosslinked by TGM, while it was much more effective for the samples without TGM, with an average improvement of 25%, though still insufficient to achieve significant water resistance.

The biodegradability of the samples was tested by treating them with protease enzyme to assess their decomposition (Table 21-SI, Fig. 5-SI and 6-SI†). Samples containing transglutaminase (CT, CS50T, CS100T, CU50T, CU100T) showed greater resistance to biodegradation than those without, particularly up to 6 hours. This effect is probably due to the covalent cross-linking induced by TGM, as previously described. After 12 hours, however, weight loss is uniform between samples with and without TGM, suggesting that the stabilization offered by TGM slows degradation only in the initial stages.

The presence of lignin in samples (CS50, CS100, CT50, CT100, CS50T, CS100T, CU50T, CU100T) appears to increase resistance to biodegradation compared to those without lignin (C and CT). This is particularly evident in samples CU50, CU100, CU50T and CU100T containing UPM lignin, which show slightly higher resistance. Increasing the lignin concentration (comparison of CU50 to CU100 or CU50T to CU100T) showed a variable impact on material stability. Considering the same

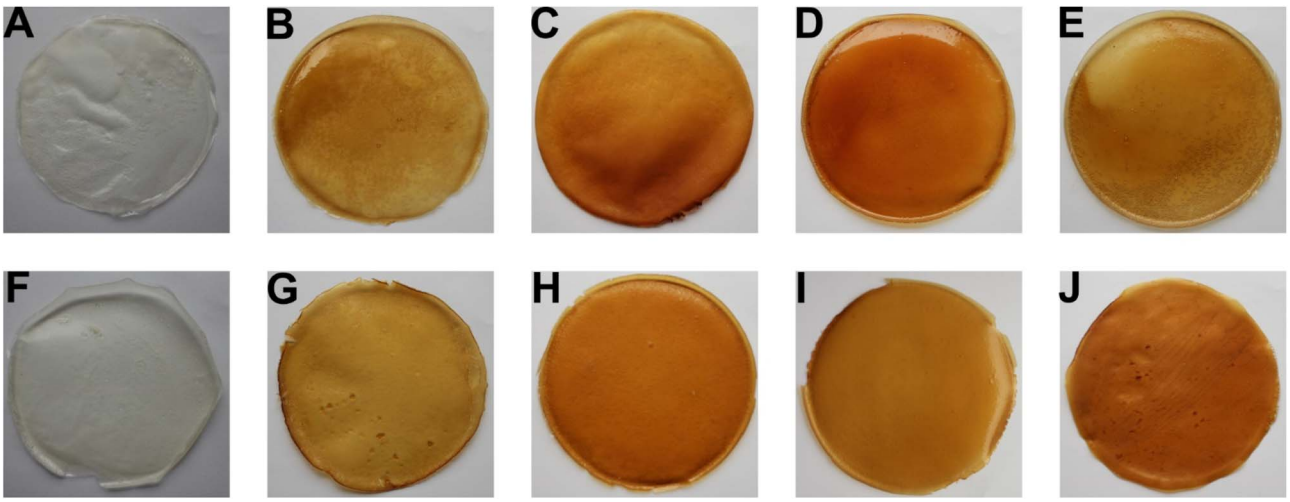

Fig. 2 Photographs of the casein-based films. (A) C, (B) CS50, (C) CS100, (D) CU50, (E) CU100, (F) CT, (G) CS50T, (H) CS100T, (I) CU50T, (J) CU100T.

Open Access Article. Published on 18 February 2025. Downloaded on 3/12/2025 4:19:18 PM. This article is licensed under a Creative Commons Attribution-NonCommercial 3.0 Unported Licence.

type of lignin, samples with 100 mg lignin (CS100 and CU100) showed no significant difference to those with 50 mg (CS50 and CU50), suggesting that there may be a limit beyond which the stabilizing effect of lignin does not increase further.

3.3.2 XRD analyses. All the XRD diffractograms acquired in the 2θ range 10–60° were identical (Fig. 7-SI†). The observed reflections are all due to KH_2PO_4, as revealed by the good match between the XRD diffractogram of CU50, taken as example, and the peaks of KH_2PO_4 indexed in the ICSD database, card 84-0328 (Fig. 8-SI†). The presence of KH_2PO_4 crystals on the surface can be explained because of the crystallization of the phosphate buffer, used in the film preparation.

Any other contributions due to the casein or other components did not appear, suggesting that the films matrix was mainly amorphous.

3.3.3 Surface analyses. The optical microscope revealed that all the samples exhibited a very similar surface, regardless of the specific composition. Fig. 9-SI† shows some images of different films acquired at 20× magnification: the surfaces were knurled but homogeneous, without clear separation of the components.

The SEM analysis (Fig. 3A and 10-SI†) showed a compact texture of the samples, without pores. The presence of lignin did not determine clear morphological differences of the surfaces. In several samples, as in the image of CS100T, geometrical areas or crystals appeared. These structures are probably caused by the crystallization of the phosphates in the buffer on the surface, as highlighted by XRD analysis. Some globular aggregates are also observable in sample containing lignin UPM; considering the very low solubility of such lignin in water, it realistically forms particles dispersed in the film matrix.

3.3.4 FT-IR. The FT-IR spectrum of the casein-based films (Fig. 3B) showed mainly the signals of the casein, previously described, and glycerol. The broad band with the maximum at 3274 cm^{-1} is remarkably intense due to the presence of several OH (humidity, glycerol); the peak at 1541 cm^{-1}, attributable to the NH bending of the casein backbone, is shifted to higher wavenumbers compared to the signal of casein alone, centred at about 1509 cm^{-1}, probably for the network interactions' effect; the C–O stretching signal at 1035 cm^{-1} is particularly strong for the presence of glycerol.

When lignin was added in the film preparation, no new signals appeared in the FT-IR spectrum: the amount of lignin was very low compared to the amounts of casein and glycerol, thus lignin absorptions were hidden.

Moreover, it was not possible to distinguish any signal of transglutaminase: being a protein, its absorptions were almost the same of casein, also its amount was at least five times smaller than the casein one.

3.3.5 Mechanical properties. On the base of the solubility results, the mechanical properties were studied only for the samples crosslinked by TGM, more resistant to water and thus more suitable for the application as a substrate for enzyme immobilization.

The mechanical properties of the different films are shown in Table 22-SI and Fig. 11-SI.†

Compared to the pure casein film, the addition of different concentrations of lignin from Sigma significantly reduces the elastic modulus (E) ($\Delta E = 20\%$) tensile stress (TS) ($\Delta TS = 33\%$), and yield strength (YS) ($\Delta YS = 29\%$) of the composite films, with the reductions becoming more pronounced as the lignin content increases ($\Delta E = 137\%$, $\Delta TS = 105\%$, $\Delta YS = 184\%$). In

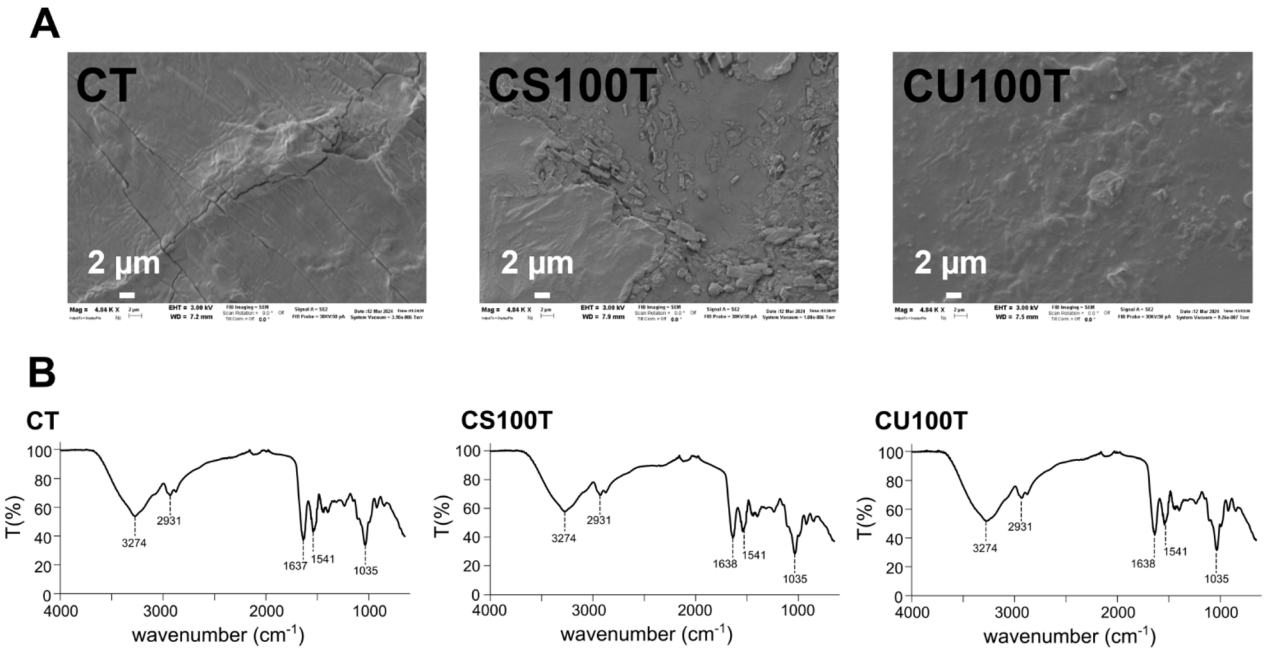

Fig. 3 (A) SEM images with SE2 detector of the samples CT, CS100T, and CU100T, (B) FT-IR of the same three samples: relevant signals are highlighted with dotted lines.

© 2025 The Author(s). Published by the Royal Society of Chemistry

Open Access Article. Published on 18 February 2025. Downloaded on 3/12/2025 4:19:18 PM.
This article is licensed under a Creative Commons Attribution-NonCommercial 3.0 Unported Licence.

contrast, the elongation at break exhibits an opposite trend, increasing with higher lignin concentrations ($\Delta\varepsilon = 31\%$).

In the case of UPM lignin, the elastic modulus and tensile stress were slightly increased by the addition of lignin, recording a variation of 17% in the case of E and 8% for TS. However, at higher lignin concentrations, a significant reduction in mechanical properties was observed (E decreases by *ca.* 300%, TS decreases by 200% and the YS by 350%) except for elongation at break for which there was an increase of *ca.* 80%. The drastic drop in the tensile strength and Young's modulus is attributed to the weak intramolecular interaction between the casein chains and to a likely agglomeration of lignin in the composites, resulting in poor stress transfer. Therefore, this decline in mechanical performance can be attributed to a less compact network structure, allowing for greater molecular mobility and consequently reducing stiffness. Lignin disperses evenly throughout the matrix and acts as a chain extender within the casein network, enhancing elongation. However, it also introduces steric hindrance, disrupting the network structure and thus lowering both tensile stress and elastic modulus.

3.3.6 LCA. The comparative LCA analysed the potential environmental impacts of a unit of film of each sample, considering all the film samples equivalent from a functional perspective. In future analyses, if focused on specific functions of interest, the LCA comparison will consider the number, mass, or dimensions of films required for each sample to achieve the same specific performance.

The LCA results (Table 23-SI†) showed that there are no substantial differences among the different samples in terms of potential environmental impacts associated with film production, with an increase of the samples impacts up to a maximum of 1% compared to the sample C.

Hotspot analyses (from Fig. 12-SI–21-SI†) were conducted to assess the contributions of different components to the overall environmental impacts of each film. The primary contributor was found to be electricity required to produce the film (>70% for 14 out of the 16 impact categories), followed by casein, and finally other added substances, which generally have a contribution lower than 5% across all the impact categories (meaning that lignin impacts are negligible). An exception to this pattern was observed in the land use impact category (Fig. 4), where casein is the dominant contributor (>75%). This is because casein environmental impact is driven by milk production, which in turn involves land occupation, maize, grain, and fertilizers as inputs. An intermediate pattern is given by the ecotoxicity, freshwater impact category, where the electricity consumption for the film production slightly exceeds the contribution of casein production.

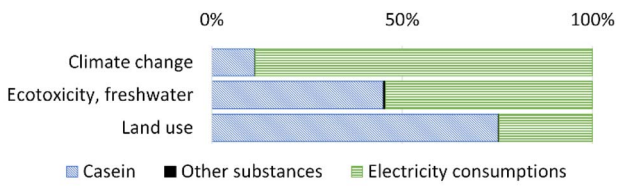

Fig. 4 Hotspot analysis for the climate change, ecotoxicity, freshwater, and land use impact categories (the graph pertains to sample C; similar patterns were observed for all the samples).

The single score potential impacts of the different samples, obtained through normalization and weighting stages (Table 24-SI†), vary from 149.3 μPt of the sample C to 149.7 μPt of the sample CU100T (Table 25-SI†).

A potential solution to mitigate environmental impacts could be the use of expired milk for casein production: as this would be a waste product, it would be burden free available.[55] In that improved scenario, the impact of casein production could be significantly reduced, with land use impact decreasing by up to 97%, and freshwater ecotoxicity by up 89%. Overall, more than a 50% reduction could be achieved across 7 out of the 16 evaluated impact categories. Under those conditions, the single score potential impacts (Table 26-SI†) would range from 140.6 μPt for sample C to 141 μPt for sample CU100T.

Moreover, it is important to note that the electricity consumptions for both casein and film production were assessed under non-optimized conditions, assuming the laboratory devices solely dedicated to these processes. In a scaled-up production scenario, optimizations could be implemented, potentially leading to further reductions in environmental impacts. In a best-case scenario, formulated considering the use of expired milk and a 50% reduction of laboratory energy consumptions (both for casein production and film production), the single score potential impacts (Table 27-SI†) would range from 70.5 μPt for sample C to 70.9 μPt for sample CU100T.

3.4 GOx-containing films

The immobilization of GOx is not new in the literature. Thin polymeric films containing GOx were widely used to functionalise electrodes to achieve the detection of glucose through amperometric biosensors.[56–59] Hanušová *et al.* immobilized GOx on polyamide and ionomer films to develop packaging materials with antimicrobial properties.[60]

The present work, however, describes a different approach: the enzyme was entrapped into the casein-based film directly during the preparation, and any toxic reagent, such as glutaraldehyde, wasn't used, because the bounding with the matrix occurred thanks to TGM, already present into the mixture. The enzyme resulted entrapped in a free-standing film, that could be cut into smaller pieces and soaked in glucose solutions. The glucose detection was then achieved through a simple colorimetric method.

The two samples of GOx-containing films were prepared following the recipe of CT and CS100T samples. The addition of glucose oxidase (GOx) to the polymeric matrix during the preparation did not affect the overall consistency, flexibility, and uniformity of the organic films containing casein (Fig. 5A) and casein with lignin (Fig. 5B). Unlike the other samples, those containing GOx were stored at 4 °C to maintain the enzyme stability and functionality.

Open Access Article. Published on 18 February 2025. Downloaded on 3/12/2025 4:19:18 PM.
This article is licensed under a Creative Commons Attribution-NonCommercial 3.0 Unported Licence.

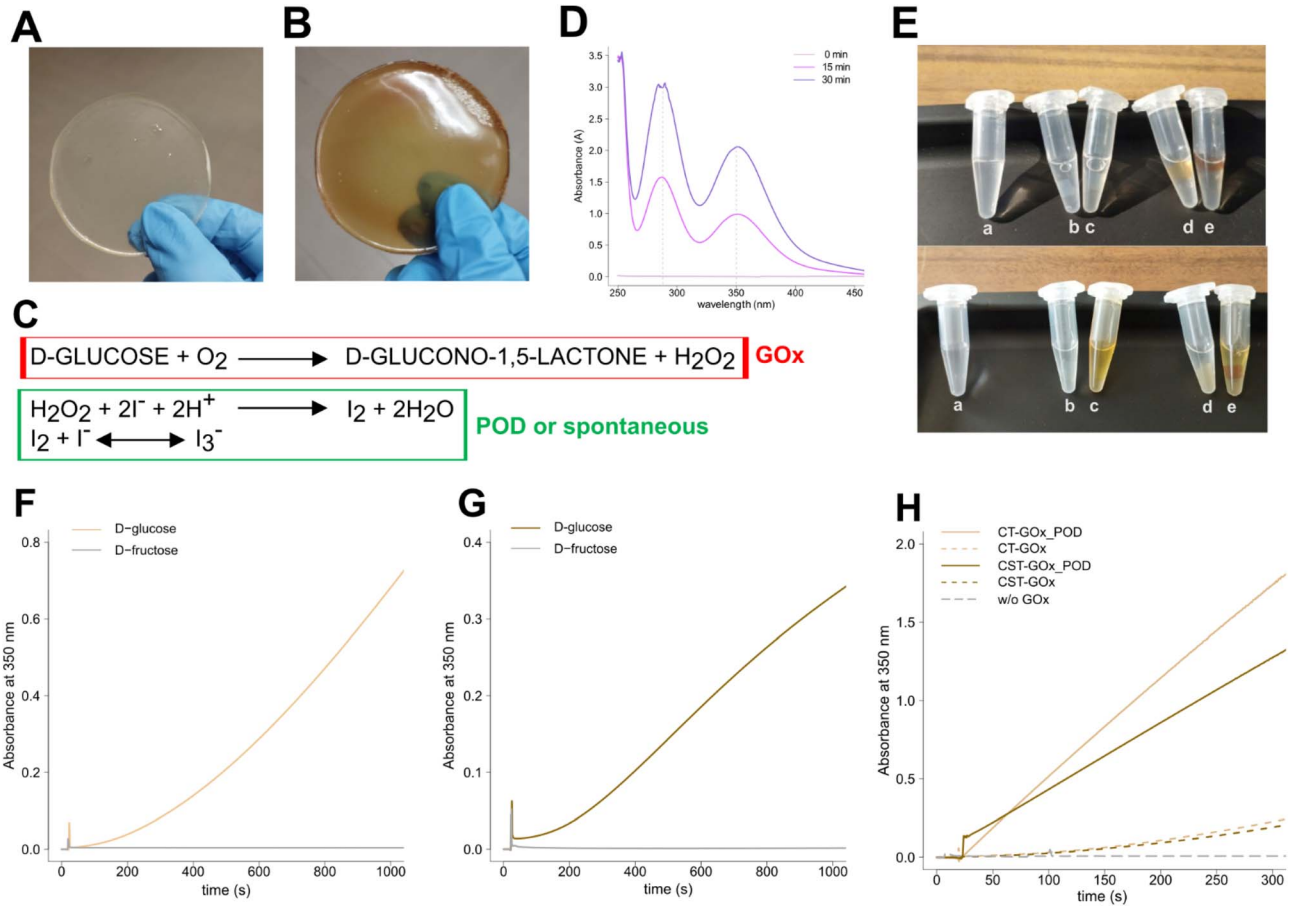

Fig. 5 Enzymatic activity of the entrapped GOx. (A) CT–GOx film entrapping 15 mg GOx. (B) CST–GOx film entrapping 15 mg GOx. (C) Schematic of the enzymatic reaction catalysed by GOx in the presence of D-glucose and oxygen (red box) and the reaction between KI and H_2O_2 that can occur spontaneously or catalysed by POD (green box). (D) Superimposed absorbance spectra acquired at different time points during the non-enzymatic reaction of H_2O_2 with KI. (E) GOx reaction was confirmed with an on-bench colorimetric assay with KI: (a) KI and D-glucose; (b) CT–GOx with KI; (c) CT–GOx with KI and D-glucose; (d) CST–GOx with KI; (e) CST–GOx with KI and D-glucose. Photographs were taken immediately after the addition of the films to the reaction tubes (top) and 30 min later (bottom). (F) Enzymatic selectivity of CT–GOx film against D-glucose and D-fructose. (G) Enzymatic selectivity of CST–GOx film against D-glucose and D-fructose. (H) Time course of I^{3-} formation at 350 nm in the presence (solid lines) and absence (dashed lines) of 5 μM POD for CT–GOx (yellow lines) and CST–GOx (brown lines) films.

The average thickness of the CT–GOx and CST–GOx films was 253 μm and 260 μm, respectively (Table 19-SI†). The resistance in water in general was worse, with a reduction of 4% and 10% for CT–GOx and CST–GOx respectively in comparison with the analogue samples without enzyme CT and CS100T (Table 20-SI†), however in PBS it was enough to perform the tests to detect glucose without dissolving the samples. The FT-IR spectra (Fig. 22-SI†) didn't reveal any difference compared to the spectra of the samples without GOx (Fig. 3). This result is predictable considering that GOx is a protein, and it was added in low amount. The SEM images (Fig. 23-SI†) showed a compact surface covered by crystalline areas due to buffer crystallization, as already observed in the samples without GOx.

The oxidase activity of the entrapped enzyme was shown to be maintained in both films by performing a chemical and an enzymatic coupled assay with POD in the presence of D-glucose and KI, which undergo a redox reaction with the H_2O_2 released from GOx (Fig. 5C), that occurs either in the presence of peroxidase or in the absence of enzymatic catalysts. The GOx reaction was confirmed by monitoring the absorbance spectrum of the reaction at different time points (Fig. 5D) since the final product, the I^3, showed an absorption spectrum with two distinct peaks at 350 nm and 290 nm.[61] The increase in the amplitude of these absorbance peaks is in fact correlated to the increase of the reaction product over time, therefore occurs as a consequence of the GOx reaction.

The colour shift occurred only after the addition of a piece of film in a solution containing both D-glucose and KI (Fig. 5E, reactions (c) and (e)) and was preliminarily observed during on-bench assays in the absence of POD; the reaction did not take place in the absence of the enzyme (Fig. 5E, reaction (a)) or D-glucose (Fig. 5E, reactions (b) and (d)). The assays performed confirmed the GOx selectivity for D-glucose and the lack of reactivity against D-fructose for both the casein-based films (Fig. 5F and G).

Since the chemical approach did not allow the comparison of the initial rates of the enzymes (Fig. 5H, dashed lines), a coupled assay with POD revealed that the GOx entrapped in

© 2025 The Author(s). Published by the Royal Society of Chemistry

Open Access Article. Published on 18 February 2025. Downloaded on 3/12/2025 4:19:18 PM. This article is licensed under a Creative Commons Attribution-NonCommercial 3.0 Unported Licence.

the casein matrix in the presence of lignin (Fig. 5H, brown solid line) appeared to be less active and is about 31% slower compared to the enzyme entrapped in the casein matrix without lignin (Fig. 5H, yellow solid line). This result was consistent with the enzymatic activity tested for the free GOx enzyme in a solution containing casein or casein and lignin (Fig. 24-SI†); in such tests, the addition of casein to the GOx solution determined a decrease in the enzymatic activity of about 9% (% calculated as $(\nu_{\text{max-noC/L}} - \nu_{\text{max-C}})/\nu_{\text{max-noC/L}} \times 100$), while the addition of lignin Sigma caused a drop of about 46%. In the presence of both casein and lignin Sigma the decrease was about 44%.

The enzymatic activity was checked over time, using different squares of the samples stored at 4 °C. The enzyme showed the higher activity against D-glucose when the samples were tested immediately after preparation; the enzymatic activity decreased significantly after three days from the preparation, with a drop of about 55% for CT–GOx and 33% for CST–GOx, however it remained still active for at least 48 days (Fig. 25-SI†). It is also important to take into account that the measurement variability for the enzymatic activities can be partially due to a plausible little difference in the enzymatic content among different squares cut from the same sample.

4. Conclusions

The present work describes the isolation by precipitation of casein from UHT skimmed milk, and the formulation and characterization of casein-based substrates, with or without two types of lignin. The resulting films exhibited a smooth and flexible texture, maintaining their stability for several months either at room temperature or at 4 °C for months.

Among the tested formulations, the presence of TGM allowed to improve the sample resistance to water, thanks to the formation of isopeptide bonds between the side chains of casein that led to the formation of a more stable protein matrix.

The addition of lignin slightly delayed the biodegradation process. Furthermore, lignin UPM contributed to a modest enhancement of the mechanical properties, leading to an increase in the elastic modulus and tensile stress. About these observations, the influence of the amount of lignin and of the kind of lignin on the film matrix will be examined more in depth in a future work.

The LCA results showed how the environmental impact of the samples could be drastically reduced starting from expired milk, in a circular economy perspective, and optimizing the experimental procedures.

GOx-containing films were prepared and tested to demonstrate that the casein-based films are suitable for enzyme entrapment: GOx remained active, even for several days, and catalysed its enzymatic reaction against D-glucose, as proved by the colorimetric detection of H_2O_2, among the reaction products. Such interesting preliminary results suggest that the described casein-based films may be potentially used as biodegradable substrates for various enzymes or macromolecules.

Data availability

The main data supporting this article have been included in the article itself or as part of the ESI;† more details are available upon request.

Author contributions

E. D. and V. S.: conceptualization, investigation, visualization, validation, writing (original draft, review & editing); G. S.: conceptualization, investigation, writing (original draft, review & editing); A. D., S. B., G. D., M. J. F. A. N.: investigation, writing (original draft, review & editing).

Conflicts of interest

There are no conflicts to declare.

Acknowledgements

Project funded under the National Recovery and Resilience Plan (NRRP), Mission 04 Component 2 Investment 1.5 – NextGenerationEU, Call for tender no. 3277 dated 30/12/2021 award number: 0001052 dated 23/06/2022. The authors thank UPM Kymmene, in particular Suvi Pietarinen, and Prof. Dominga Rogolino (University of Parma) who kindly provided UPM lignin, César De Julián Fernández (CNR-IMEM) who provided Sigma lignin, Paolo Dambruoso (CNR-ISOF) for the help with NMR measurements, Manuele Bettelli (CNR-IMEM) for the help with the optical microscope analyses, Patrizia Ferro and Marco Villani (CNR-IMEM) for their help with XRD analyses, and Tamara Posati (CNR-ISOF) for the scientific support and the useful suggestions.

References

1 A. Haug, A. T. Høstmark and O. M. Harstad, *Lipids Health Dis.*, 2007, **6**, 25.
2 P. Walstra, *J. Dairy Sci.*, 1990, **73**(8), 1965–1979.
3 M. R. Ginger and M. R. Grigor, *Comp. Biochem. Physiol., Part B:Biochem. Mol. Biol.*, 1999, **124**, 133–145.
4 M. Guetouache, B. Guessas and S. Medjekal, *Issues Biol. Sci. Pharmaceut. Res.*, 2014, **2**(10), 115–122.
5 D. A. Goulding, P. F. Fox and J. A. O'Mahony, *Milk Proteins*, ed. M. Boland and H. Singh, Academic Press, 3rd edn, 2020, ch. 2, pp. 21–98, ISBN 9780128152515.
6 W. N. Eigel, J. E. Butler, C. A. Ernstrom, H. M. Farrell, V. R. Harwalkar, R. Jenness and R. McL. Whitney, *J. Dairy Sci.*, 1984, **67**(8), 1599–1631.
7 D. S. Horne, *Milk Proteins*, ed. M. Boland and H. Singh, Academic Press, 3rd edn, 2020, ch. 6, pp. 213–250, ISBN 9780128152515.
8 M. R. Khan, S. Volpe, M. Valentino, N. A. Miele, S. Cavella and E. Torrieri, *Coatings*, 2021, **11**, 899.
9 M. L. Picchio, Y. G. Linck, G. A. Monti, L. M. Gugliotta, R. J. Minari and C. I. A. Igarzabal, *Food Hydrocoll.*, 2018, **84**, 424–434.

© 2025 The Author(s). Published by the Royal Society of Chemistry

Open Access Article. Published on 18 February 2025. Downloaded on 3/12/2025 4:19:18 PM. This article is licensed under a Creative Commons Attribution-NonCommercial 3.0 Unported Licence.

10 V. Chaudhary, P. Kajla, P. Kumari, S. P. Bangar, A. Rusu, M. Trif and J. M. Lorenzo, *Front. Nutr.*, 2022, **9**, 942524.
11 F. Song, L. M. Zhang, J. F. Shi and N. N. Li, *Colloids Surf., B*, 2010, **79**(1), 142–148.
12 E. Khodaverdi, S. Maftouhian, A. Aliabadi, M. H.-K. F. Mohammadpour, B. Khameneh and F. Hadizadeh, *J. Pharm. Invest.*, 2019, **49**, 635–641.
13 L. G. L. Nascimento, F. Casanova, N. F. N. Silva, A. V. N. Teixeira and A. F. D. Carvalho, *Food Chem.*, 2020, **314**, 126063.
14 Y. Yang, Q. Xu, X. Wang, Z. Bai, X. Xu and J. Ma, *Food Chem.*, 2024, **447**, 138956.
15 Q. Zhu, X. Zhou, Y. Zhang, D. Ye, K. Yu, W. Cao, L. Zhang, H. Zheng, Z. Sun, C. Guo, X. Hong, Y. Zhu, Y. Zhang, Y. Xiao, T. G. Valencak, T. Ren and D. Ren, *Biomater. Res.*, 2023, **27**, 6.
16 L. V. Garcia, D. Silva, M. M. Costa, H. Armés, M. Salema-Oom, B. Saramago and A. P. Serro, *Pharmaceutics*, 2023, **15**, 334.
17 J. Ahmed, E. Guler, G. S. Ozcan, M. E. Cam, S. Homer-Vanniasinkam and M. Edirisinghe, *J. R. Soc. Interface*, 2023, **20**, 0166.
18 D. Kolahreez, L. Ghasemi-Mobarakeh, F. Quartinello, F. W. Liebner, G. M. Guebitz and D. Ribitsch, *Biomacromolecules*, 2024, **25**(2), 700–771.
19 N. D. V. Raydan, L. Leroyer, B. Charrier and E. Robles, *Molecules*, 2021, **26**, 7617.
20 M. Guo and G. Wang, *Polymers*, 2016, **8**, 324.
21 L. Guan, S. Yan, X. Liu, X. Li and G. Gao, *J. Mater. Chem. B*, 2019, **7**, 5230.
22 E. De Gregorio, F. M. Miliani, F. M. Vivaldi, N. Calisi, N. Poma, A. Tavanti, C. Duce, F. Nardella, S. Legnaioli, A. G. Carota, L. Strambini, D. Biagini, T. Lomonaco, F. Di Francesco and P. Salvo, *Mater. Chem. Phys.*, 2024, **314**, 128888.
23 A. M. Boudet, *Plant Physiol. Biochem.*, 2000, **38**(1–2), 81–96.
24 S. Sugiarto, Y. Leow, C. L. Tan, G. Wang and D. Kai, *Bioact. Mater.*, 2022, **8**, 71–94.
25 D. S. Bajwaa, G. Pourhashemb, A. H. Ullahb and S. G. Bajwac, *Ind. Crops Prod.*, 2019, **139**, 111526.
26 F. Vásquez-Garay, I. Carrillo-Varela, C. Vidal, P. Reyes-Contreras, M. Faccini and R. A. T. Mendonça, *Sustainability*, 2021, **13**, 2697.
27 O. Yu and K. H. Kim, *Appl. Sci.*, 2020, **10**, 4626.
28 M.-L. Mattinen, G. Riviere, A. Henn, R. W. N. Nugroho, T. Leskinen, O. Nivala, J. J. Valle-Delgado, M. A. Kostiainen and M. Österberg, *Nanomaterials*, 2018, **8**(12), 1001.
29 T. C. Krishna, A. Najda, A. Bains, M. M. Tosif, R. Papliński, M. Kapłan and P. Chawla, *Polymers*, 2021, **13**, 3164.
30 J. C. Buzby, H. F. Wells and J. Hyman, *U.S. Department of Agriculture, Economic Research Service, Economic Information Bulletin*, 2014, vol. **121**, pp. 1–33.
31 M. Eriksson, I. Strid and P.-A. Hansson, *Resour., Conserv. Recycl.*, 2014, **83**, 44–52.
32 V. Leskovac, S. Trivić, G. Wohlfahrt, J. Kandrač and D. Peričin, *Int. J. Biochem. Cell Biol.*, 2005, **37**(4), 731–750.
33 M. H. Hassan, C. Vyas, B. Grieve and P. Bartolo, *Sensors*, 2021, **21**, 4672.
34 H. Teymourian, A. Barfidokht and J. Wang, *Chem. Soc. Rev.*, 2020, **49**, 7671.
35 J. Wang, *Chem. Rev.*, 2008, **108**(2), 814–825.
36 N. Palermo, V. Buffagni, F. Vurro, G. Impollonio, D. Pignone, M. Janni, H. T. Nguyen, E. Dembech and N. Marmiroli, *Environ. Exp. Bot.*, 2024, **228**(A), 105986.
37 R. D'Orsi, C. V. Irimia, J. J. Lucejko, B. Kahraman, Y. Kanbur, C. Yumusak, M. Bednorz, F. Babudri, M. Irimia-Vladu and A. Operamolla, *Adv. Sustainable Syst.*, 2022, **6**, 2200285.
38 C. Gazzurelli, M. Carcelli, P. P. Mazzeo, C. Mucchino, A. Pandolfi, A. Migliori, S. Pietarinen, G. Leonardi, D. Rogolino and P. Pelagatti, *Adv. Sustainable Syst.*, 2022, **6**, 2200108.
39 U. K. Laemmli, *Nature*, 1970, **227**(5259), 680–685.
40 M. R. Khan, S. Volpe, E. Salucci, M. B. Sadiq and E. Torrieri, *J. Food Eng.*, 2022, **335**, 111190.
41 M. Barbalinardo, M. Giannelli, L. Forcini, B. Luppi, A. Donnadio, M. L. Navacchia, G. Ruani, G. Sotgiu, A. Aluigi, R. Zamboni and T. Posati, *Int. J. Mol. Sci.*, 2022, **23**, 6805.
42 International Organization for Standardization ISO, *ISO 14040: Environmental management – Life cycle assessment – Principles and framework (ISO 14040:2006+ Amd1:2020)*, 2006a.
43 International Organization for Standardization ISO, *ISO 14044: Environmental management – Life cycle assessment – Requirements and guidelines (ISO 14044:2006+Amd1:2017+Amd2:2020)*, 2006b.
44 S. A. Bassi, F. Biganzoli, N. Ferrara, A. Amadei, A. Valente, S. Sala and F. Ardente, *Updated Characterisation and Normalisation Factors for the Environmental Footprint 3.1 Method*, Publications Office of the European Union, 2023.
45 Ecoinvent Centre, *Ecoinvent Version 3.10 Database*, 2023, accessed 16th September 2024, available at: **https://ecoinvent.org/ecoinvent-v3-10/**.
46 D. P. Ballou, I. S. Isaac and J. H. Dawson, *Essays Biochem.*, 1999, **34**, 51–69.
47 R. C. Bateman Jr and J. A. Evans, *J. Chem. Educ.*, 1995, **72**(12), A240.
48 M. Morrison, G. S. Bayse and A. W. Michaels, *Anal. Biochem.*, 1971, **42**(1), 195–201.
49 T. Pojanavaraphan, R. Magaraphan, B. S. Chiou and D. A. Schiraldi, *Biomacromolecules*, 2010, **11**(10), 2640–2646.
50 A. A. Hassanin, A. Osman, O. O. Atallah, M. T. El-Saadony, S. A. Abdelnour, H. S. A. Taha, M. F. Awad, H. Elkashef, A. E. Ahmed, I. Abd El-Rahim, A. Mohamed and A. S. Eldomiaty, *Front. Vet. Sci.*, 2022, **9**, 952319.
51 H. Bouzid, M. Rabiller-Baudry, L. Paugam, F. Rousseau, Z. Derriche and N. E. Bettahar, *J. Membr. Sci.*, 2008, **314**(1–2), 67–75.
52 L. T. Kakalis, T. F. Kumosinski and H. M. Farrell, *Biophys. Chem.*, 1990, **38**(1–2), 87–98.
53 T. Markoska, D. Daniloski, T. Vasiljevic and T. Huppertz, *Molecules*, 2021, **26**(24), 7650.

© 2025 The Author(s). Published by the Royal Society of Chemistry

Open Access Article. Published on 18 February 2025. Downloaded on 3/12/2025 4:19:18 PM.
This article is licensed under a Creative Commons Attribution-NonCommercial 3.0 Unported Licence.

54 K. Vasić, Ž. Knez and M. Leitgeb, *Int. J. Mol. Sci.*, 2023, **24**(15), 12402.
55 The International EPD® System, *General Programme Instructions, Version 4.0*, 2021, accessed 26th September 2024, available at: **https://www.datocms-assets.com/37502/1617181375-general-programme-instructions-v-4.pdf**.
56 T. Homma, T. Ichimura, M. Kondo, T. Kuwahara and M. Shimomura, *Eur. Polym. J.*, 2014, **51**, 130–135.
57 T. Y. Uzumer, S. Cete, Y. Tekeli and E. E. Altuner, *Biotechnol. Appl. Biochem.*, 2024, **71**, 1440–1452.
58 M. Shimomura, R. Miyata, T. Kuwahara, K. Oshima and S. Miyauchi, *Eur. Polym. J.*, 2007, **43**(2), 388–394.
59 A. L. Sharma, R. Singhal, A. Kumar, Rajesh, K. K. Pande and B. D. Malhotra, *J. Appl. Polym. Sci.*, 2004, **91**, 3999–4006.
60 K. Hanušová, L. Vápenka, J. Dobiáš and L. Mišková, *Cent. Eur. J. Chem.*, 2013, **11**, 1066–1078.
61 M. Wang, S. Qiu, H. Yang, Y. Huang, L. Dai, B. Zhang and J. Zou, *Chemosphere*, 2021, **270**, 129448.